Characteristic vertical profile of plume injection from wild-land fires

Sofiev[1], M., Vankevich[2], R., Ermakova[2], T.

[1] Finnish Meteorological Institute, Helsinki, Finland

[2] Russian State Hydrometeorological University, St.Petersburg, Russia

1 Abstract

A problem of a characteristic vertical profile of the smoke released from wild-land fires is considered. A methodology for bottom-up evaluation of this profile is suggested and a corresponding global dataset is calculated. The profile estimation is based on: (i) a semi-empirical formula for plume-top height recently suggested by the authors, (ii) MODIS satellite observations of active wild-land fires, and (iii) meteorological conditions evaluated at each fire place using the output fields of a numerical weather prediction model. Plumes from fires recorded globally during two arbitrarily picked years 2001 and 2008 are evaluated and their smoke injection profiles are calculated with a time step of 3 hours. The resulting 4-dimensional dataset is projected to global grid with resolution $1^o \times 1^o \times 500$m, averaged to monthly level, and normalised. Evaluation of the created dataset was performed at several levels. Firstly, the quality of the semi-empirical formula for plume-top computations was evaluated using the MISR plume height dataset. Secondly, the obtained maps of the injection profiles are compared with another global distribution available from literature. Finally, the stability of the calculated profiles with regard to inter-annual variations of the fire activity is roughly evaluated by comparing the sub-sets for 2001 and 2008.

Key words: emission injection profile, wild-land fires, plume rise

2 Introduction

Wild-land fires is one of the major contributors of trace gases and aerosols to the atmosphere. The fire smoke affects the air chemical and physical properties at a wide range of spatial and temporal scales, which are directly related to lifetime of the released pollutants in the atmosphere. In turn, removal and chemical transformations of these species strongly depend on the altitude of their injection in the atmosphere. The bulk of the fire smoke is released in the atmospheric boundary layer (ABL) [*Val Martin et al.*, 2010; *Sofiev et al.*, 2012, 2009] but strong fires occurring under favourable atmospheric conditions can send the plumes high into the free troposphere (FT) [*Freitas et al.*, 2007; *Labonne et al.*, 2007] and up to the stratosphere, where the smoke can stay for long time

and spread over very large areas [*Dirksen et al.*, 2009; *Fromm et al.*, 2000; *Luderer et al.*, 2006]. Therefore, it is of crucial importance for both climate- and atmospheric composition- related applications to reproduce the vertical profiles of the fire plumes.

Most of atmospheric composition models distribute the fire emissions homogeneously starting from the ground up to prescribed plume-top height H_p, which is sometimes region-dependent. For global chemistry-transport models, *Davison*, [2004], *Forster et al.*, [2001], *Liousse et al.*, [1996] set it to about 2 km, whereas for regional simulations of smoke from intense Canadian fires *Westphal and Toon*, [1991] used 5–8 km. *Lavoué et al.*, [2000] showed that H_p is usually about 2–3 km for fires in the northern latitudes, but can reach 7–8 km for powerful crown fires. The biomass burning in Central America is usually less intense, therefore $H_p \sim 0.9–1.5$ km was suggested by *Kaufman et al.*, [2003]. Following this estimation, *Wang et al.*, [2006] used 1.2 km (8th model layer) for the mesoscale simulations and conducted sensitivity studies showing 15% variation of the near-surface concentrations if H_p is varied plus-minus one model layer (a few hundreds of meters). An estimation of typical injection height from fires for Northern America was performed by *Val Martin et al.*, [2010] using MISR plume height observations. There, the inter-annual variability, relation to vegetation type, as well as seasonal dependence were demonstrated using statistics of over 3300 plumes.

More accurate approaches for the fire injection height computations suggested by *Freitas et al.*, [2007], *Lavoué et al.*, [2000], and *Sofiev et al.*, [2012] are based on explicit accounting for the features of individual fires and actual ambient atmospheric conditions. These methods provide better representation of the plume vertical distribution but share the same weakness: application of the methodologies requires quite detailed information for each fire. This information is not available if the emission estimates are based on burnt-area data or aggregated in time and space (e.g. the widely used Global Fire Emission Dataset GFED, [*van der Werf et al.*, 2006]). Therefore, there is a need for pre-calculated “typical” injection profile from wild-land fires, which can be used in practical applications if the detailed fire information is not available or too bulky to be used [*Dentener et al.*, 2006].

The goal of the current work is to estimate the characteristic injection vertical profile of the wild-land fire plumes over the globe and to determine its seasonal and spatial variations.

In the following section we outline the input methodology, formalises the problem and describes the input datasets; section 5 describes the preparatory steps and additional evaluation of the methodologies involved. Section 6 presents the outcome of the calculations, whereas section 7 compares it with another dataset and analyses some features of the obtained profiles.

3 Materials and methods

3.1 Methodology for evaluation of fires emission plumes

Calculation of the characteristic injection profile will be based on recently suggested semi-empirical formula for the fire-plume top height [*Sofiev et al.*, 2012]. According to

this methodology, the plume-top H_p depends on the Fire Radiative Power *FRP*, height of the atmospheric boundary layer ABL, H_{abl}, and Brunt-Vaisala frequency in the free troposphere N_{FT}:

(1) $$H_p = \alpha H_{abl} + \beta \left(\frac{FRP}{P_{f0}} \right)^{\gamma} \exp(-\delta N_{FT}^2 / N_0^2)$$

Coefficients α, β, γ, and δ, and normalising constants P_{f0} and N_0 are:

(2) $$\alpha = 0.24; \quad \beta = 170\ m; \quad \gamma = 0.35; \quad \delta = 0.6; \quad P_{f0} = 10^6 W, \quad N_0^2 = 2.5 * 10^{-3} s^{-2}$$

3.2 Formalisation of the problem for determination of the characteristic vertical profile of fire emission

Problem statement

Let intensities of fires $\{f_i, i=1..N_f\}$ are observed by a satellite instrument when the spacecraft overpasses the burning area at times $\{\tau_j, j=1..N_\tau\}$. The result of the observation is recorded as a radiation power $P_{fi}(\tau_j)$ for each fire f_i and overpass time τ_j. A collection of the meteorological data is available from a meteorological model as time- and space-dependent variables: ABL height $H_{ABL}(x,y,t)$, and the FT Brunt-Vaisala frequency $N^2(x,y,z,t)$.

The goal is to evaluate the gridded monthly-mean vertical distribution of the fire emission:

(3) $$e(i, j, k, m), \quad i = 1..I, \quad j = 1..J, \quad k = 1..K, \quad m = 1..12, \quad \sum_{k=1}^{K} e(i, j, k, m) = 1,$$

where *I,J,K* are the *x*-, *y*-, and *z*- wise dimensions of the grid, *i,j,k* are corresponding indices, and *m* is month number.

Problem solution.

Following [*Sofiev et al.*, 2009], a linear relation of the fire intensity and its emission rate can be assumed. With the plume-top H_p dependence on the fire and meteorological parameters (1), it leads to the following distribution density of the emitted species during the lifetime of one fire *f*:

(4) $$\frac{\partial E_f}{\partial z}(x_f, y_f, z) = s_e(x_f, y_f) \int_T P_f(t) \frac{\partial E}{\partial z}(H_p(t), z)\, dt,$$

where s_e is the emission factor converting P_f to the emission rate of particular species, x_f and y_f are the fire coordinates, and $\frac{\partial E}{\partial z}$ is the universal vertical distribution density of emission from individual fire, which depends only on the plume top height H_p. For the

determination of $\frac{\partial E}{\partial z}$, following *Briggs*, [1975], the plume thickness is taken equal to height of its centreline H_C, sp that $H_p = 1.5H_C$. Distribution of the emitted masses is then taken homogeneous from $0.5H_p$ up to H_p.

Having the emission distribution from a single fire (4) computed for all fires, the needed monthly gridded distribution in each grid cell *(i,j)* can be obtained via summation over all fires f_m that occurred within its borders during each month *m*:

(5)
$$\frac{\partial e}{\partial z}(i,\ j, z, m) = \frac{\sum_{f_m} \frac{\partial E_f}{\partial z}(z)}{\int_0^{\infty} \sum_{f_m} \frac{\partial E_f}{\partial z}(z)\, dz}$$

For the finite-thickness vertical layer *k*, which extends from $z_{k-1/2}$ till $z_{k+1/2}$, finally obtain:

(6)
$$e(i,\ j, k, m) = \int_{z_{k-1/2}}^{z_{k+1/2}} \frac{\partial e}{\partial z}(i,\ j, z, m)\, dz$$

The problem is therefore reduced to computation of the eq (4) for each fire in the dataset.

The simplest case considered further is computation of vertical distribution for the total fire emission (sum over all species). According to *Sukhinin et al.*, [2005], the fire radiative power P_f is linearly connected with the burnt fuel and, following *Kaufman et al.*, [1998], with the total amount of the released trace gases and aerosols. For such a case, the emission factor s_e is independent from the land-use type and therefore is cancelled out during the normalization step (5).

For each individual species this coefficient is land-use and fire-type dependent, which makes the consideration of the full integral (4) for all stages of the fire development inevitable. As a result, the mean distribution will be specific for each species. Emission factors can be taken from the Integrated System for wild-land fires (IS4FIRES, *Sofiev et al.*, [2009]) for total PM and re-scaled to other species following *Andreae and Merlet*, [2001]. However, inter-relations of these coefficients are very uncertain and dependent on the fire type and state, i.e. also time-dependent. With limited fire information available and large uncertainties of the methodologies, this extra complexity of the computations is not justified. Therefore, below the profiles were computed for total emission only.

3.3 Input data for the plume computations

The information on the wild-land fires intensity needed for the above methodology is obtained from the active-fire observations by MODIS instrument onboard Aqua and Terra satellites (http://modis.gsfc.nasa.gov). The MODIS collection 5 of the active fire characteristics includes both radiative temperatures of the overheated pixel and its surrounding background pixels and emission rate of the radiative energy from the pixel, the Fire Radiative Power (FRP, [W]). This dataset is essentially the only existing

collection that covers the whole globe over more than a decade (the Terra satellite was launched in 2000, Aqua in 2002) and provides information on active fires rather than on the burnt area.

FRP products have recently become available also from geostationary satellites, such as MSG SEVIRI [*Kaiser et al.*, 2009; *Roberts and Wooster*, 2008]. Large pixel size of such satellites (more than 10×10 km^2) precludes their direct utilization since such pixel often covers many individual fires. However, high temporal resolution (15 min for SEVIRI) makes them a valuable source of information about the temporal evolution of the total fire intensity.

The meteorological information over the globe is taken from the operational archives of the Integrated Forecasting System (IFS) of European Centre for Medium-Range Weather Forecast (ECMWF). The Brunt-Vaisala frequency was computed directly from vertical temperature profile. The ABL height was estimated by the dry-parcel method, which performance was evaluated and compared with other approaches by *Sofiev et al.*, [2006].

The plume-rise formulations (1)-(2) have been evaluated for boreal and mid-latitude fires by [*Sofiev et al.*, 2012], which is insufficient for the purposes of this work. Therefore, additional evaluation was performed based on the observations of the MISR Plume Height Project [*Kahn et al.*, 2008; *Mazzoni et al.*, 2007]. For the current study we used all information available to-date, which included injection heights for about 2500 fires that took place in the US, Canada, Siberia, Africa, and Borneo during 2005–2009.

4 Preparatory steps for the profile calculations

Before starting the computations, several preparations have to be made: (i) to perform additional evaluation of the plume-rise formula for (sub-) tropical regions, (ii) to develop a method for determination of the temporal evolution of the fire intensity, and (iii) select the method for filling-in the gaps in the obtained dataset.

4.1 Global evaluation of the plume rise formula

The global-scale evaluation of the formulations (1)-(2) is based on new MISR data, which were not available for the original study [*Sofiev et al.*, 2012]. New MISR datasets for Africa and Borneo allow for extension of the original boreal- and temperate-forest evaluation towards savannah and tropical forests.

The evaluation task, contrary to the original parameter identification problem, does not pose strict demand to the data amount. Therefore, we considered only so-called “good” plume height retrievals of MISR, for which the accuracy of the plume-top retrieval is the highest. This selection reduces the size of the dataset from about 2500 fire cases down to 1650 cases, which is sufficient for the evaluation task.

The comparison of predictions of formula (1)-(2) with MISR observations (Figure 1) confirms the main conclusion of the original evaluation by [*Sofiev et al.*, 2012]: the parameterization is able to predict the top height of >70% of the fire plumes within 500m from the MISR observations. For Borneo the fraction of good predictions appeared to be even higher: above 90%. Therefore, the formulations (1)-(2) can be used over the whole

globe with quite homogeneous quality of predictions: over two-thirds of the plumes are within 500m form the observations. Some details of the formulation performance are further discussed in section 7.

4.2 Estimation of the temporal evolution of fire intensity and meteorological parameters

Estimating the diurnal evolution of the fire intensity $P_f(t)$ using observations of low-orbit satellite, such as MODIS, is not feasible. Two or four overpasses during a day, even if not obscured by clouds, are insufficient to resolve this variation. However, computation of evolution of each fire is not needed for the purposes of this study. Average diurnal variation would be sufficient: correlation between the meteorological and fire developments will be captured, whereas specifics of individual fires will be averaged out during the normalization step.

Estimation of the diurnal variation of fire intensity is a comparatively straightforward task if based on fire products from geostationary satellites [*Roberts and Wooster*, 2008; *Roberts et al.*, 2009]. We used the outcome of spectral analysis of the FRP time series obtained from MSG SEVIRI by J.Hakkarainen (personal communication), from where the hourly variation coefficients $p(h)$, $h=1..24$ were calculated from the Fourier-transform coefficients (Table 1).

The coefficients $p(h)$ represent the diurnal variation of total FRP over the SEVIRI pixel P_{seviri}. However, large SEVIRI pixels usually cover many fires, so that the intensity of the individual fires $P_{fpix\,i}$ and their total number $N_{f\,pix}$ ($i=1..N_{f\,pix}$)within the given pixel are convoluted into a single variable:

$$P_{seviri} = \sum_{i=1}^{N_{fpix}} P_{f\,i} \qquad (7)$$

Generally speaking, both $N_{f\,pix}$ and $P_{f\,i}$ vary during a day. For smaller pixels of low-orbit (LEO) satellites, the number $N_{f\,pix}$ is also small, so that the variation of the number of fires is explicitly resolved as variation of the number of overheated pixels [*Roberts et al.*, 2009]. With MODIS data, however, this signal suppressed by few overpasses during a day, cloud obstruction and other uncertainties. For another LEO satellite TRMM the situation is better, owing to its nearly-equatorial orbit [*Roberts et al.*, 2009]. However, inter-relations of SEVIRI and TRMM variations are hard to establish, which makes deconvolution of the eq (7) using TRMM data highly uncertain. Therefore, for the current analysis it is assumed that the SEVIRI-based diurnal variation (Table 1) is applicable for the pixels of MODIS.

4.3 Spatial interpolation and gap closure

The bottom-up approach of the profile computations has one significant drawback: there are areas where no fires took place during some months of the analysed years. Such holes in the map have to be filled-in from the surrounding grid cells with similar land-use, providing that those exist. No extrapolation beyond the area with fires seems is justified.

Since in many regions the number of fires per pixel (Figure 2) for specific month was quite limited, noise reduction attempt was made by running 3D low-pass filtration followed by renormalization. However, below the results are presented without this filtration step in order to preserve the variability of the injection height for different land use types.

5 Results

The results of the computations comprise 12 global monthly 3-D distributions of the fire total emission, which are available from http://is4fires.fmi.fi.

Spatial pattern of the vertical injection profile highlights several regions with particularly low and particularly high fires (Figure 3). Most of high plumes were predicted for forested regions of Northern and Southern America and Eurasia, which agrees with general expectations that the strong fires are more probable in the areas with the highest fuel load. Particularly high fires occurred in Australia, probably owing to frequent droughts occurring in that region. Equatorial African fires, to the opposite, appeared to generate quite low plumes: the bulk of mass was injected in the lowest 1-2km. Noteworthy, the evaluation for African savannahs (Figure 1) suggested certain over-estimation of the plume top height (see the discussion section), therefore the actual injection profile may be positioned even lower.

Zonally-averaged vertical profile (Figure 4) shows similar picture: in equatorial region, where the bulk of contribution is from African savannah fires, the top of the injection profile is lower than in the forested middle latitudes.

From the Figure 4 one can also see that the record-high fires actually have little connection to the bulk of the emission: over the globe more than 50% of the fire emission is confined with in the lowest 1-2km, i.e. within the atmospheric boundary layer.

6 Discussion

6.1 Systematic biases of the plume top formula

Additional evaluation of the plume-top formulations (1)-(2) highlighted the tendency of the parameterization to over-state the height of low plumes with certain under-estimation of the high ones. For the African dataset this resulted in a high bias of ~150m, owing to significant fraction of low plumes (H_p < 700m) over-stated by the parameterization. For Borneo, where the fires were more powerful and plumes generally went above 700m, the agreement was very good: bias was less than 30m and >90% of the plumes were predicted within 500m from the observations.

A potential explanation of this tendency is that the grass fires usually occupy wide areas, so that the FRP density, $[W\ m^{-2}]$, is substantially lower than that for the forest fires – despite the total FRP can be comparable. The present formulations do not take this into

account due to high uncertainty of the fire area estimations and their practically unknown shape (position of the fire fronts, temperature distribution over the burn area, etc.). As a result, predicted plume top for a wide but low-FRP-density fire will be the same as that for a concentrated limited-size event – providing that the total FRPs and meteorological conditions are the same. In reality, the plume from a concentrated fire seems to be injected higher, which causes the above tendency.

The other uncertainty of the approach is connected with a time period needed for the plume to reach its top position. Since MISR and MODIS are both onboard of Terra, their observations have the same time stamp. However, the plume position corresponds to FRP of the fire as it was some 15-30 minutes ago. This can lead to up to 20-30% of difference in the FRP value (if estimated from the parameters of Table 1), i.e. bring a few tens of metres difference to the H_p prediction.

6.2 Representativeness of the obtained profiles for individual episodes

The current profiles have been obtained from the analysis of two distant years – 2001 and 2008. These two years provided sufficient coverage ensuring that no region is missed from the maps (Figure 3). Still, the number of fire events for specific months can be fewer than 10 for about 10-20% of grid cells (Figure 2). For these areas the results of the current computations should be taken with care.

A quantitative estimation of representativeness of the obtained results can be obtained from comparison of the results for individual years. Their representativeness can be roughly estimated by splitting the considered years and comparing the individual estimates (Figure 5). Expectedly, one can see that the 90^{th} percentile for August shown in Figure 5 varied between the years, with more powerful fires recorded in 2008 in both Northern and Southern America, whereas in Eurasia and Africa the plumes were higher in 2001. This observation points out at importance of dynamic plume estimations, wherever they are available: even at monthly averaging the difference of actual injection height and average one can reach several hundreds of metres.

6.3 Seasonal variations of the injection profiles

Importance of the monthly resolution of the injection profile is demonstrated in Figure 6. One can see that the hemispheric-mean values of FRP and ABL height follow quite similar seasonal curves with peaks in warm months. As a result, the mean height of 90^{th} percentile of injection profile also shows 30-40% of seasonal variation. This result is in qualitative agreement with [*Val Martin et al.*, 2010] results for Northern America.

Correlation of the ABL top and plume injection heights leads to fairly constant fraction of the fire smoke emitted inside the ABL throughout the year: slightly less than half of total mass (50% height of the 50^{th} percentile in Figure 6 is close but higher than the ABL height). This fraction agrees well with statistics of [*Val Martin et al.*, 2010] and can also be related to the 85% of the total number of fire plumes confined inside the ABL [*Sofiev et al.*, 2009]. Comparing these fractions, one can conclude that about 15% of the most-

powerful fires bring about 50% of the smoke emission into the free troposphere – and this fraction does not change significantly throughout the year.

The seasonal variations of the profiles should be superposed with their diurnal cycle. Variation of FRP by more than a factor of two between day and night (Table 1), being correlated with diurnal cycle of ABL height, evidently brings about comparable or even more significant variation of the vertical emission profile. It is therefore highly advisable to take these high-frequency fluctuations into account in practical applications.

6.4 Comparison with Aerocom

In the introduction section, it was noted that in most of practical applications the injection profiles are taken very crudely. We are aware about only one spatially-resolving map of mean injection top recommended for AEROCOM (Aerosol Comparisons between Observations and Models) community by *Dentener et al.*, [2006] (Figure 6). That work, however, did not explain how the map was obtained. Comparison with the results of the present study reveals a few similarities but also several differences between the estimates.

Among the similarities, one can notice the western part of Northern America, where both datasets suggest quite high fires routinely reaching 3km and, according to the present study, even exceeding this level. Agreement exists also over Oceania and part of Australia, where the height of 90% of the mass injection is close to the top height recommended for AEROCOM.

For Southern America the datasets show significantly different patterns: current assessment has not registered high plumes over the eastern coast and in the south, instead reporting them in the forest regions in the middle of the continent. With no independent estimates available for the region, it is hard to make a definite choice. However, in the densely populated coastal regions the wild-land fires should be controlled tighter than in the barely inhabited tropical forest, so that the probability for strong fires should be lowering towards the populated regions. Noteworthy, the number of fires cases clearly decreases towards the coast (Figure 2), which is partly due to less dense vegetation in the cultivated regions and, probably, due to tighter control of the fires.

Patterns over Eurasia and Australia demonstrate the shift between the maps. The highest plumes in AEROCOM map are attributed to semi-desert areas of Australia and tundra in Northern Eurasia. According to MODIS, there were no fires registered there during the considered years. These regions are also characterised by low fuel load and, in case of Northern Eurasia, frequent occasions of thin boundary layer. Therefore, it seems quite unlikely to have particularly high plumes over these regions.

Rare fires over Scandinavia can hardly release the smoke high above the ground either: the forests are closely monitored and maintained there, so that the fires are quickly extinguished. Our data for that region showed very few events with typical injection under 2km.

7 Summary

The presented dataset is the result of bottom-up computations of characteristic vertical profiles of the wild-land fires smoke. It is obtained by processing the records of active fires by MODIS instrument onboard of Aqua and Terra satellites. The analysis covered two years – 2001 and 2008, – the whole globe and resulted in monthly 3D maps of injected fraction of the fire smoke.

The computations showed that the highest plumes reaching up to 6-8 km are characteristic for forested areas, whereas grassland fires usually emit within the lowest 2-3km. Over the globe, about 50% of the fire emission is injected within the lowest 1-2km, i.e. is confined inside the atmospheric boundary layer.

The dataset is publicly open at http://is4fires.fmi.fi.

8 Acknowledgements

The study has been performed within the TEKES – KASTU 2 project. Support of EU FP7 PASODOBLE project is kindly appreciated. MODIS and MISR satellite data were obtained from public online databank of NASA.

9 References

Andreae, M. O., and P. Merlet (2001), Emission of trace gases and aerosols from biomass burning, *Global biogeochemical cycles*, *15*(4), 955-966.

Briggs, G. A. (1975), Plume rise predictions, in *Lectures on air pollution and environmental impact analyses*, pp. 59-111, Boston.

Davison, P. S. (2004), Estimating the direct radiative forcing due to haze from the 1997 forest fires in Indonesia, *Journal of Geophysical Research*, *109*(D10), 1-12, doi:10.1029/2003JD004264. [online] Available from: http://www.agu.org/pubs/crossref/2004/2003JD004264.shtml (Accessed 11 August 2011)

Dentener, F. et al. (2006), Emissions of primary aerosol and precursor gases in the years 2000 and 1750 prescribed data-sets for AeroCom, *Atmospheric Chemistry and Physics*, *6*, 4321-4344. [online] Available from: www.atmos-chem-phys.net/6/4321/2006/

Dirksen, R. J., K. Folkert Boersma, J. de Laat, P. Stammes, G. R. van der Werf, M. Val Martin, and H. M. Kelder (2009), An aerosol boomerang: Rapid around-the-world transport of smoke from the December 2006 Australian forest fires observed from space, *Journal of Geophysical Research*, *114*(D21), 1-15, doi:10.1029/2009JD012360. [online] Available from:

http://www.agu.org/pubs/crossref/2009/2009JD012360.shtml (Accessed 11 August 2011)

Forster, C. et al. (2001), Transport of boreal forest fire emissions from Canada to Europe, *Journal of Geophysical Research*, *106*(D19), 22887-22906, doi:10.1029/2001JD900115. [online] Available from: http://www.agu.org/pubs/crossref/2001/2001JD900115.shtml

Freitas, S. R., K. M. Longo, R. Chatfield, D. Latham, M. a. F. Silva Dias, M. O. Andreae, E. Prins, J. C. Santos, R. Gielow, and J. a. Carvalho (2007), Including the sub-grid scale plume rise of vegetation fires in low resolution atmospheric transport models, *Atmospheric Chemistry and Physics*, *7*(13), 3385-3398, doi:10.5194/acp-7-3385-2007. [online] Available from: http://www.atmos-chem-phys.net/7/3385/2007/

Fromm, M., A. Jerome, K. Hoppel, J. Hornstein, R. Bevilacqua, E. Shettle, R. Servranckx, L. Zhanqing, and B. Stocks (2000), Observations of boreal forest fire smoke in the stratosphere by POAM III, SAGE II, and lidar in 1998, *Geophysical Research Letters*, *27*(9), 1407-1410, doi:10.1029/1999GL011200. [online] Available from: http://www.agu.org/pubs/crossref/2000/1999GL011200.shtml

Kahn, R. A., Y. Chen, D. L. Nelson, F.-Y. Leung, Q. Li, D. J. Diner, and J. A. Logan (2008), Wildfire smoke injection heights: Two perspectives from space, *Geophysical Research Letters*, *35*(4), 4-7, doi:10.1029/2007GL032165. [online] Available from: http://www.agu.org/pubs/crossref/2008/2007GL032165.shtml (Accessed 11 August 2011)

Kaiser, J. W., M. J. Wooster, G. Roberts, M. G. Schultz, G. V. D. Werf, and A. Benedetti (2009), SEVIRI Fire Radiative Power and the MACC Atmospheric Services, in *EUMETSAT Meteorological Satellite Conf., ISBN 978-92-9110-086-6, ISSN 1011-3932*, pp. 2005-2009, EUMETSAT,, Darmstadt, Germany.

Kaufman, I. ., M. . Steele, D. L. Cummings, and V. J. Jaramillo (2003), Biomass dynamics associated with deforestation, fire, and, conversion to cattle pasture in a Mexican tropical dry forest, *Forest Ecology and Management*, *176*(1-3), 1-12.

Kaufman, Y. J., C. O. Justice, L. P. Flynn, J. D. Kendall, E. Prins, L. Giglio, D. E. Ward, P. Menzel, and A. Setzer (1998), *Potential global fire monitoring from EOS-MODIS*. [online] Available from: http://www.cstars.ucdavis.edu/papers/html/kaufmanetal1998a/index.html

Labonne, M., F.-M. Bréon, and F. Chevallier (2007), Injection height of biomass burning aerosols as seen from a spaceborne lidar, *Geophysical Research Letters*, *34*(11), 1-5, doi:10.1029/2007GL029311. [online] Available from: http://www.agu.org/pubs/crossref/2007/2007GL029311.shtml (Accessed 11 August 2011)

Lavoué, D., C. Liousse, H. Cachier, B. J. Stocks, and J. G. Goldammer (2000), Modeling of carbonaceous particles emitted by boreal and temperate wildfires at northern latitudes, *Journal of Geophysical Research*, *105*(D22), 26871-26890, doi:10.1029/2000JD900180. [online] Available from: http://www.agu.org/pubs/crossref/2000/2000JD900180.shtml

Liousse, C., J. E. Penner, C. Chuang, J. J. Walton, H. Eddleman, and H. Cachier (1996), A global three-dimensional model study of carbonaceous aerosols, *Journal of Geophysical Research*, *101*(D14), 19411-19432, doi:10.1029/95JD03426. [online] Available from: http://www.agu.org/pubs/crossref/1996/95JD03426.shtml

Luderer, G., J. Trentmann, T. Winterrath, C. Textor, M. Herzog, H. F. Graf, and M. O. Andreae (2006), Modeling of biomass smoke injection into the lower stratosphere by a large forest fire (Part II): Sensitivity studies, *Atmospheric Chemistry and Physics*, *6*, 5261-5277, doi:doi:10.5194/acp-6-5261- 30 2006. [online] Available from: http://www.atmos-chem-phys-discuss.net/6/6081/2006/

Martin, M. Val, J. a. Logan, R. A. Kahn, F.-Y. Leung, D. L. Nelson, and D. J. Diner (2010), Smoke injection heights from fires in North America: analysis of 5 years of satellite observations, *Atmospheric Chemistry and Physics*, *10*(4), 1491-1510, doi:10.5194/acp-10-1491-2010. [online] Available from: http://www.atmos-chem-phys.net/10/1491/2010/

Mazzoni, D., J. A. Logan, D. Diner, R. a. Kahn, L. Tong, and Q. Li (2007), A data-mining approach to associating MISR smoke plume heights with MODIS fire measurements, *Remote Sensing of Environment*, *107*, 138-148.

Roberts, G. J., and M. J. Wooster (2008), Fire Detection and Fire Characterization Over Africa Using Meteosat SEVIRI, *IEEE Transactions on Geoscience and Remote Sensing*, *46*(4), 1200-1218, doi:10.1109/TGRS.2008.915751. [online] Available from: http://ieeexplore.ieee.org/lpdocs/epic03/wrapper.htm?arnumber=4469869

Roberts, G., M. J. Wooster, and E. Lagoudakis (2009), Annual and diurnal african biomass burning temporal dynamics, *Biogeosciences*, *6*(5), 849-866, doi:10.5194/bg-6-849-2009. [online] Available from: http://www.biogeosciences.net/6/849/2009/

Sofiev, M., T. Ermakova, and R. Vankevich (2012), Evaluation of the smoke-injection height from wild-land fires using remote-sensing data, *Atmospheric Chemistry and Physics*, *12*(4), 1995-2006, doi:10.5194/acp-12-1995-2012.

Sofiev, M., P. Siljamo, I. Valkama, M. Ilvonen, and J. Kukkonen (2006), A dispersion modelling system SILAM and its evaluation against ETEX data, *ATMOSPHERIC ENVIRONMENT*, *40*(4), 674-685, doi:10.1016/j.atmosenv.2005.09.069.

Sofiev, M., R. Vankevich, M. Lotjonen, M. Prank, V. Petukhov, T. Ermakova, J. Koskinen, and J. Kukkonen (2009), An operational system for the assimilation of the satellite information on wild-land fires for the needs of air quality modelling and forecasting, *Atmospheric Chemistry and Physics*, *9*(18), 6833-6847.

Sukhinin, A. I., S. G. Conard, D. J. McRae, G. A. Ivanova, P. A. Tsvetkov, V. A. Bychkov, and O. A. Slinkina (2005), Remote Sensing of Fire Intensity and Burn Severity in Forests of Central Siberia, in *Contemporary Problems of Earth Remote Sensing from Space*, Space Research Institute RAS., Mscow. [online] Available from: http://www.iki.rssi.ru/earth/ppt2005/sukhinin.pdf

Wang, J., S. a. Christopher, U. S. Nair, J. S. Reid, E. M. Prins, J. Szykman, and J. L. Hand (2006), Mesoscale modeling of Central American smoke transport to the United States: 1. "Top-down" assessment of emission strength and diurnal variation impacts, *Journal of Geophysical Research*, *111*(D5), 1-21, doi:10.1029/2005JD006416. [online] Available from: http://www.agu.org/pubs/crossref/2006/2005JD006416.shtml (Accessed 11 August 2011)

Werf, G. R. van der, J. T. Randerson, L. Giglio, G. J. Collatz, P. S. Kasibhatla, and A. F. Arellano Jr. (2006), Interannual variability in global biomass burning emissions from 1997 to 2004, *Atmospheric Chemistry and Physics*, *6*, 3423-3441.

Westphal, L., and O. B. Toon (1991), Simulations of Microphysical, Radiative, and Dynamical Processes in a Continental-Scale Forest Fire Smoke Plume, *Journal of Geophysical Research*, *96*(D12), 22379-22400, doi:10.1029/91JD01956. [online] Available from: http://www.agu.org/pubs/crossref/1991/91JD01956.shtml

Table 1. Mean diurnal variation of FRP obtained from spectral analysis of SEVIRI FRP data.

Fourier coefs	a_0	a_1	a_2	b_1	b_2
Values	86.93	-56.08	12.74	-27.68	13.97

Figure captions

Figure 1. Global-scale evaluation for plume top formulations of *Sofiev et al.*, [2012a]**.**

Figure 2. Number of fires in February and August recorded by MODIS, sum of 2001 and 2008.

Figure 3. Injection top height for 50%^{h} (left) and 90% (right) of mass for February (top) and August (bottom). Unit = [m].

Figure 4. Zonal average of the vertical injection profile, August.

Figure 5. Injection top height for 90% of mass for 2001 (left) and 2008 (right). Unit = [m]

Figure 6. Seasonality of the injection height, Northern Hemisphere (left), Southern Hemisphere (right). Unit = [m].

Figure 7. Map of the plume top recommended by *Dentener et al.*, [2006]. Unit=[m]. Adopted from the online paper version.

Temperate and boreal fires, North America and Siberia, 2007-2009, 1321 plumes, “good quality retrievals”	(Sub-) tropical savannah, Africa, 2005-2006, 181 plumes, “good quality” retrievals	Tropical forest, Borneo, 2006, 2009, 144 plumes, “good quality” retrievals.

Figure 1. Global-scale evaluation for plume top formulations of *Sofiev et al.*, [2012a].

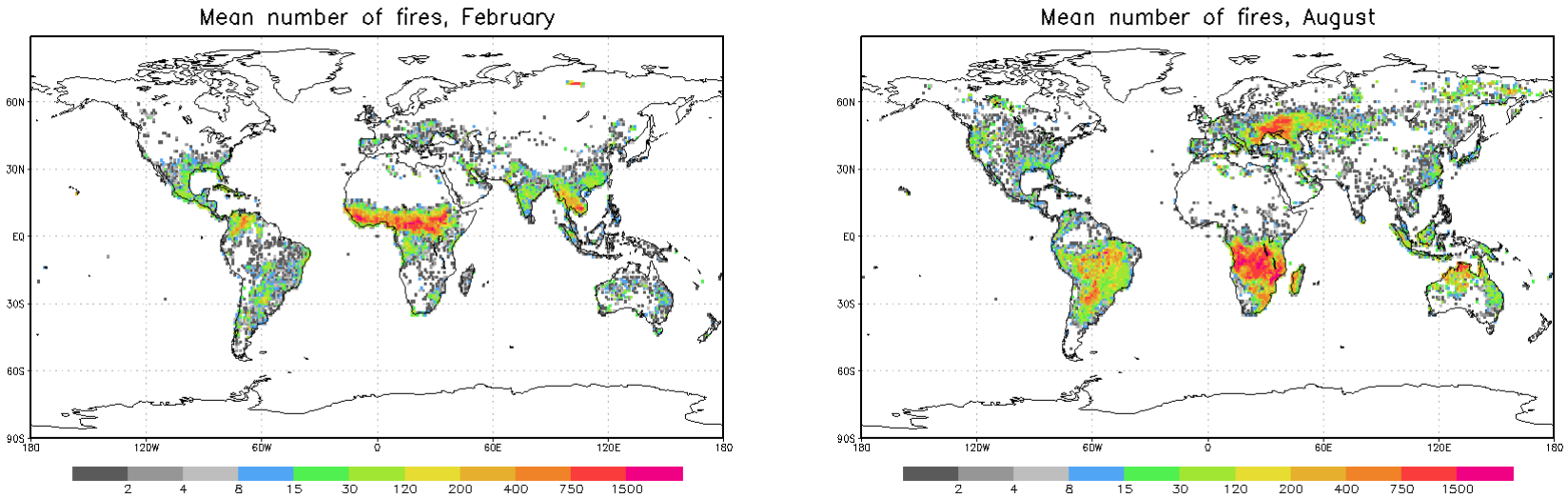

Figure 2. Number of fires in February and August recorded by MODIS, sum of 2001 and 2008.

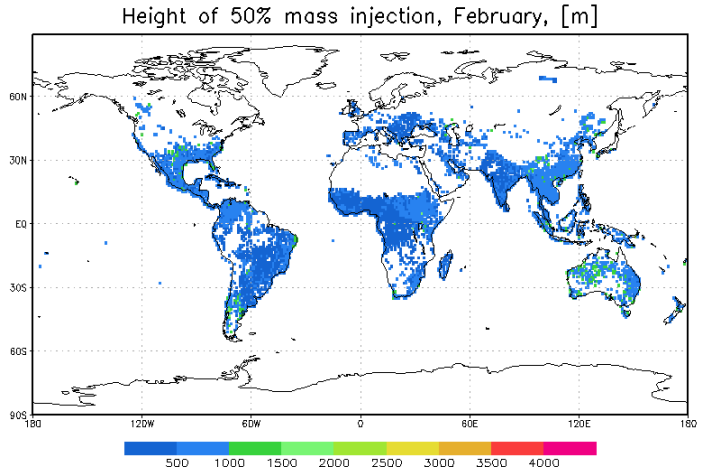

a)

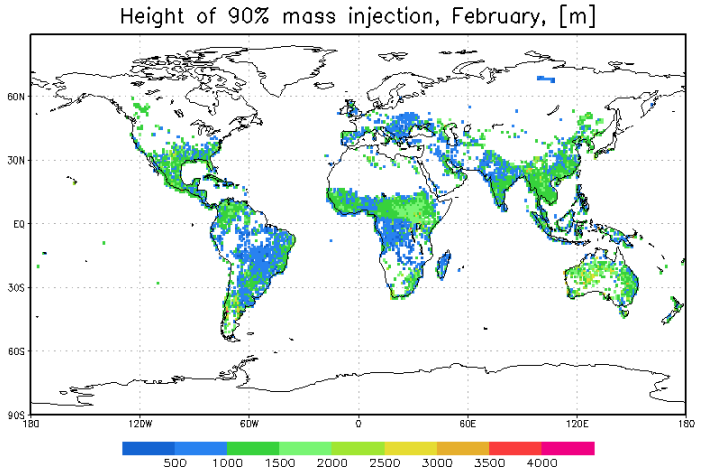

b)

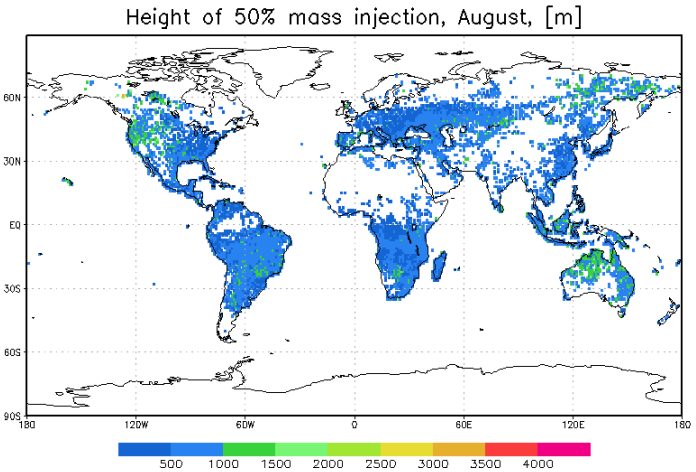

c)

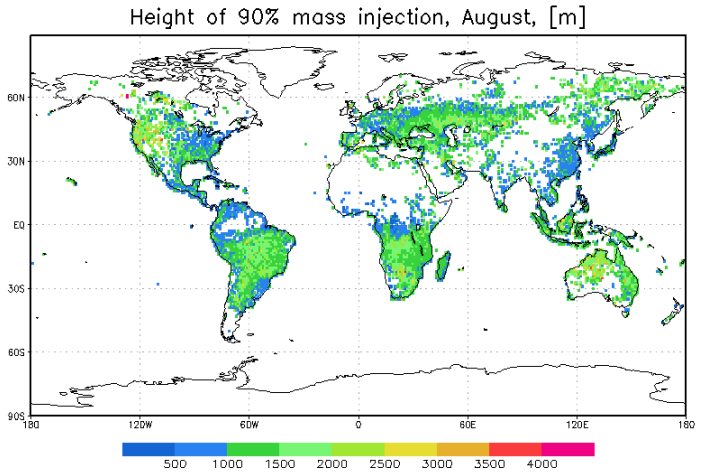

d)

Figure 3. Injection top height for 50%h (left) and 90% (right) of mass for February (top) and August (bottom). Unit = [m].

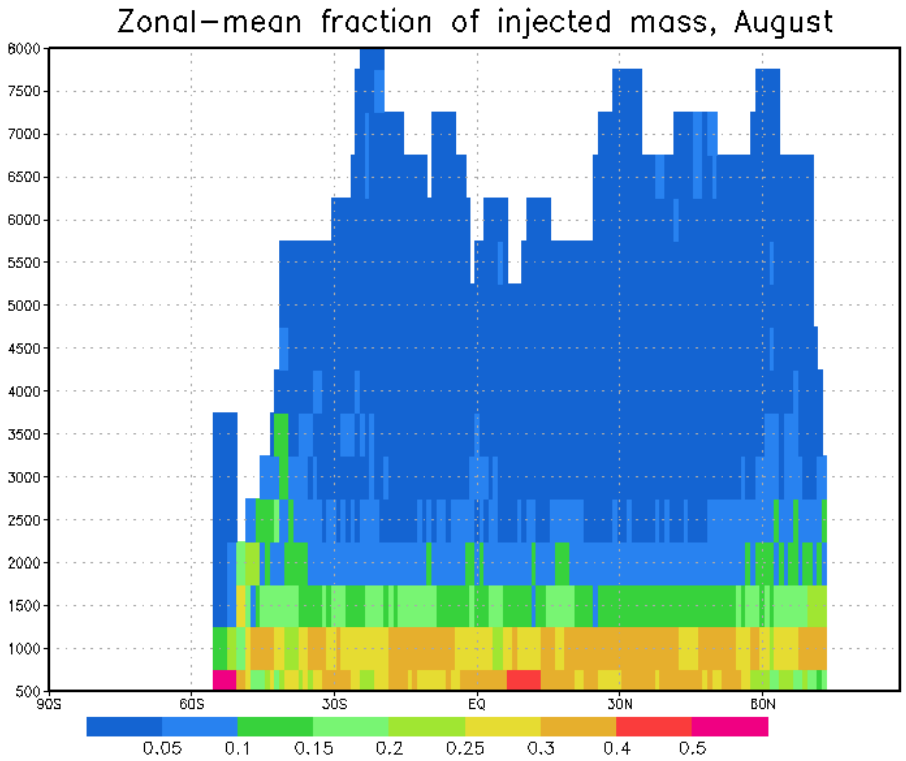

Figure 4. Zonal average of the vertical injection profile, August.

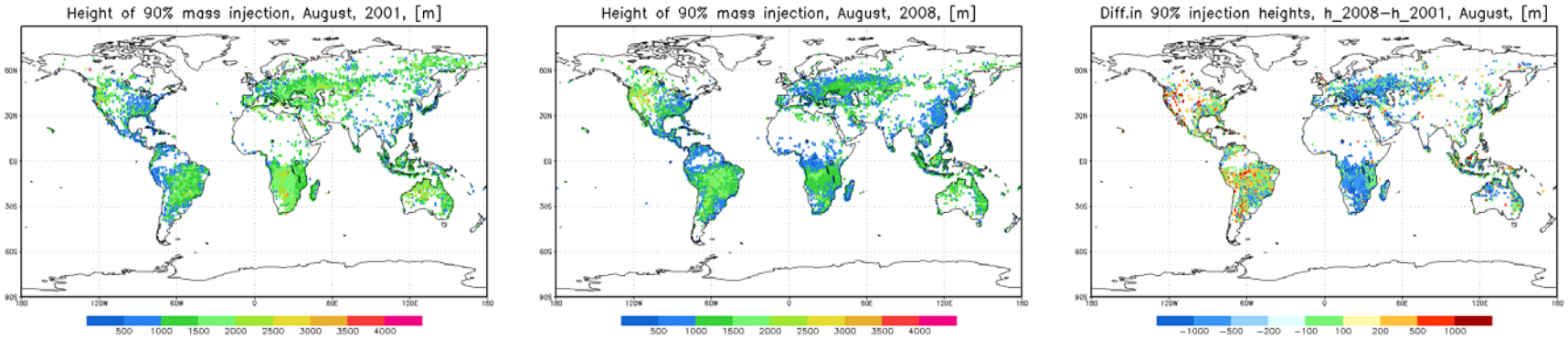

Figure 5. Injection top height for 90% of mass for 2001 (left) and 2008 (right). Unit = [m]

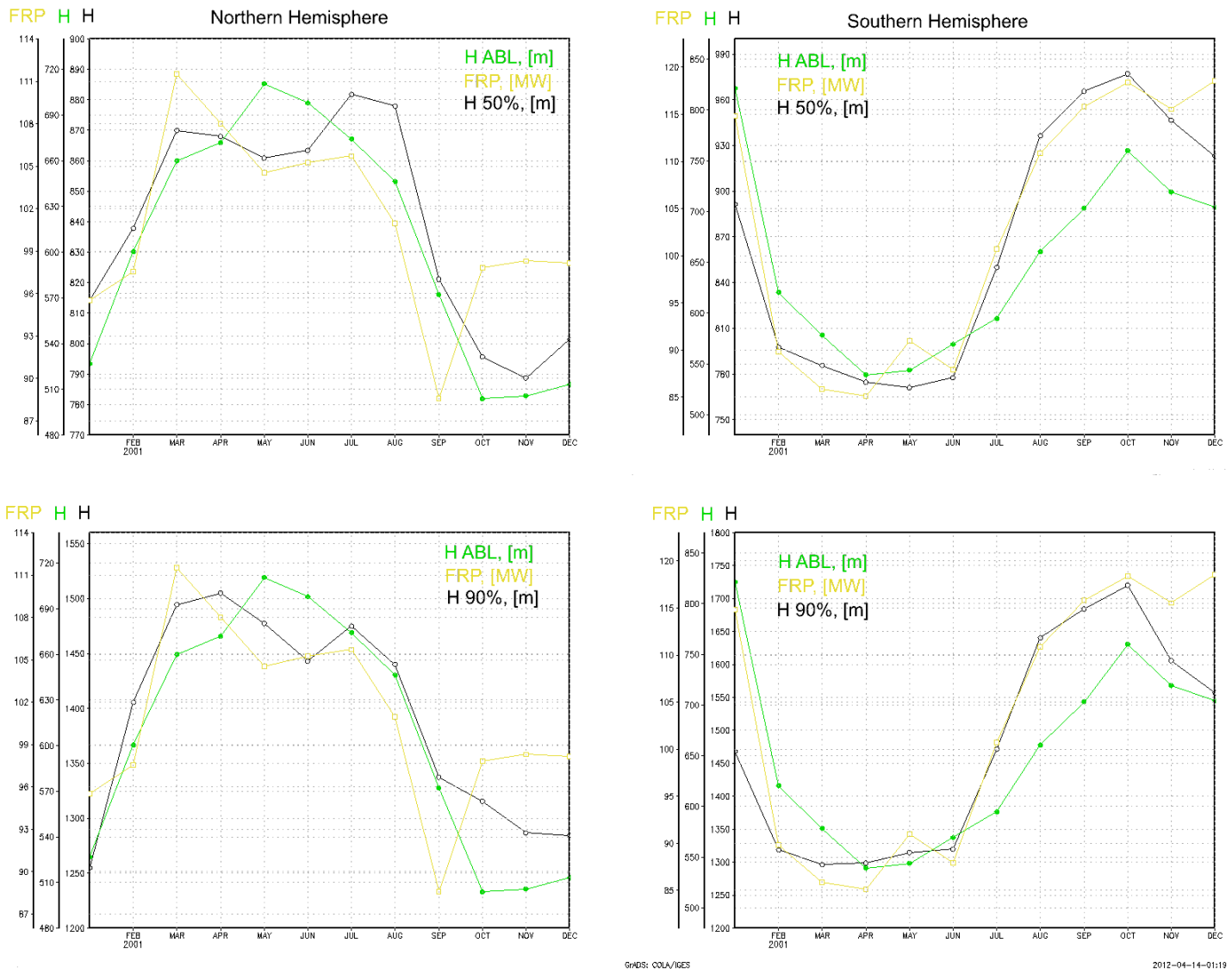

Figure 6. Seasonality of the injection height, Northern Hemisphere (left), Southern Hemisphere (right). Unit = [m].

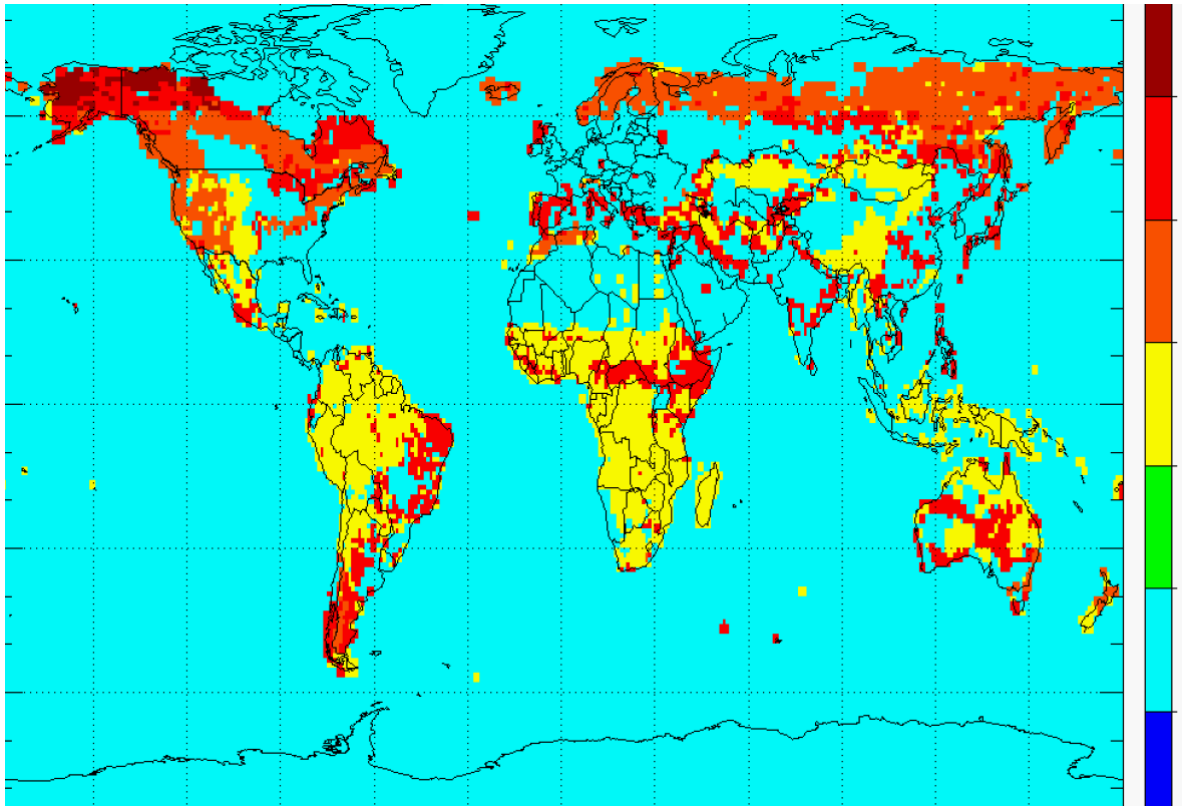

Figure 7. Map of the plume top recommended by *Dentener et al.*, [2006]. Unit=[m]. Adopted from the online paper version.